Proceedings of the ASME 2013 International Design Engineering Technical Conferences and Computers and Information in Engineering Conference
IDETC/CIE 2013
August 4-7, 2013, Portland, Oregon, USA

DETC2013-13462

EARLY-STAGE DESIGN OF RHEOLOGICALLY COMPLEX MATERIALS VIA MATERIAL FUNCTION DESIGN TARGETS

N. Ashwin Bharadwaj, James T. Allison, Randy H. Ewoldt
University of Illinois at Urbana-Champaign
Urbana, IL 61801
Email: nkbhara2@illinois.edu, jtalliso@illinois.edu, ewoldt@illinois.edu

ABSTRACT

Rheological material properties are high-dimensional function-valued quantities, such as frequency-dependent viscoelastic moduli or non-Newtonian shear viscosity. Here we describe a process to model and optimize design targets for such rheological material functions. For linear viscoelastic systems, we demonstrate that one can avoid specific a priori assumptions of spring-dashpot topology by writing governing equations in terms of a time-dependent relaxation modulus function. Our approach embraces rheological design freedom, connecting system-level performance to optimal material functions that transcend specific material classes or structure. This technique is therefore material agnostic, applying to any material class including polymers, colloids, metals, composites, or any rheologically complex material. These early-stage design targets allow for broadly creative ideation of possible material solutions, which can then be used for either material-specific selection or later-stage design of novel materials.

1 Introduction

Engineers most commonly design with hard materials or simple fluids, but the advantages of soft material design are widely demonstrated by biological systems, in which nonlinear viscoelastic properties are exploited for functionality. For example, strain-stiffening of artery walls enables stability to inflation over a range of pressures [1] and the dramatic viscous shear-thinning of snail pedal mucus (the biopolymer gel slime trail) enables wall-climbing adhesive locomotion [2]. Such nonlinear rheology has been used to design a wall-climbing robot (Robosnail) [3, 4], but rheologically complex materials are not a standard part of the engineering design toolbox.

We see two main challenges that have inhibited engineers from using nonlinear viscoelastic materials to achieve design functionality. First, the *complexity* of viscoelastic materials is a major challenge for systematic design. Even the simplest material properties are *functions*, not constants. Second, when design efforts do involve soft materials, the work is often focused on a specific material class (polymers, colloids, etc.). This focus is extremely important for rational design of material systems, and is a (later stage) component of the overall design process (Figure 1). However, focusing only on a specific material class limits the creative design space, since various material classes might give the same rheological functionality desired. This idea is central to the early-stage of the design process (Figure 1), where a target specification (functionality) should be stated in a way that is independent of the various concepts (material formulations) that may achieve it. As outlined by Cussler and Moggridge [5], "it is the [functionality] - not the molecule that produces the [functionality] - that is important." For example, viscoelastic functionality may come from polymers, colloids, and many other forms of structured soft materials. An early stage material-agnostic approach places fewer structural restrictions on the design space, and may help avoid design fixation [6].

Here we develop a design process that is material-agnostic during the early stages of optimal target setting, and material-specific during concept generation and selection (Figure 1). This brings a system-level perspecive to an area otherwise focused on

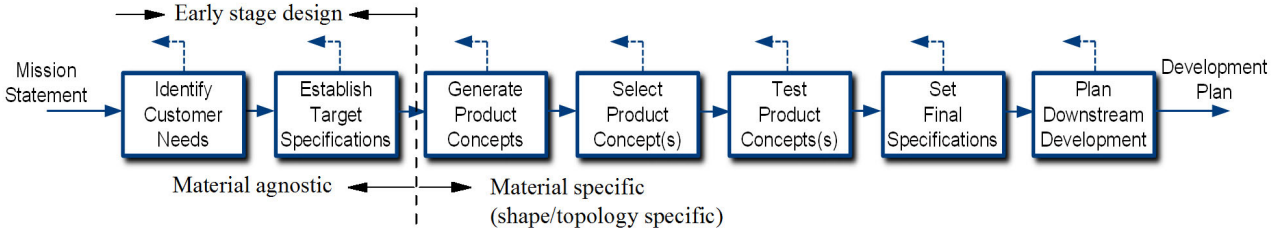

Figure 1: Different stages of the product design process that can be applied to rheologically-complex materials (design process adapted from Ulrich and Eppinger [7]).

material-class-specific research. The hierarchy in our problem separately connects functional performance to rheological properties and rheological properties to material formulation. Such hierarchical problems can be tackled efficiently using optimization techniques such as analytical target cascading (ATC) [8, 9] or inductive design exploration methods [10].

In this work we outline a modeling methodology for using material functions as system-level variables at varying levels of material specificity and deformation complexity. We then use optimization methods to solve rheological material target problems at varying levels of design freedom. These general tools and methodologies will be broadly applicable to design involving rheologically complex soft materials. We demonstrate the utility of the new tools and methodologies with an example of viscoealstic vibration attenuation.

2 Background

2.1 Rheological material functions are not necessarily constitutive equations

Rheological properties are distinct from many other material properties because they are function-valued quantities, e.g. transient shear viscosity $\eta^+(t,\dot{\gamma})$ which depends on both shear rate amplitude $\dot{\gamma}$ and time t. Because they are function-valued, rheological properties are known as material functions. True material functions are defined independently from any constitutive model, and can be applied to any material. These descriptive measures include linear viscoelastic moduli $G'(\omega)$ and $G''(\omega)$, transient shear viscosity $\eta^+(t,\dot{\gamma})$, and many other measures [11].

Material functions underlie our understanding of rheology, forming the universal language for describing rheological material responses. This language is the starting point to describe intensive material responses to various loading conditions, but they are not, in general, predictive models in themselves. Descriptive material functions are used for conceptually understanding material responses, for connecting and inferring the composition and microstructure of a material, and serve as a conceptual starting point for developing and testing constitutive equations that can predict material responses under more complex deformations.

We hypothesize that there exists a large class of modeling scenarios for which equivalence can be made between material functions and model parameters, enabling design freedom in terms of material functions. This would enable design targets to be set in the universal language of material functions, independent of constitutive model or material type. These targets would then be used to generate a wide range of concepts for different material classes that could achieve the desired rheological functionality. We describe scenarios for this correspondence in Section 3.

2.2 Functionality-driven design process

Prior work exists in the realm of functionality-driven viscoelastic material design. Some work involves the design of viscoelastic passive dampers, but without frequency dependence [12], and therefore limited design freedom. Viscoelasticity is in general time (or frequency) dependent. Time-dependent viscoelastic material design has been considered by Hilton [13–15]. These works consider integral constitutive models of linear viscoelastic behavior, at times involving both time-varying and spatially-varying properties. Viscoelastic functions are quantitatively described by a superposition of exponentials, rather than arbitrary functions. This can limit the design freedom, since this structural form cannot include a delta function (instantaneous damping) and the series representation may require a large number of parameters to describe analytically simple relaxation functions such as power-law relaxation. Mathematical models are discussed in [13–15], but numerical optimization routines are not implemented.

3 A Modeling Methodology

Our focus in this work lies in the early stages of the design process (Figure 1). At present, there is no systematic approach to modeling directly with material functions, i.e. modeling with material-agnostic function-valued quantities that can universally describe any material class. Starting from the highest abstraction (and design freedom), here we seek a methodology to model rheological elements in terms of (i) arbitrary force trajectories,

(ii) material functions with arbitrary functional form, (iii) material functions with specified analytical forms, and (iv) specific constitutive models. At the highest level we will replace rheological elements with arbitrary force trajectories. This embodies the most design freedom, and may give insight about optimal targets, since such force trajectories can be optimized [16, 17]. After gaining this insight, more specificity must be considered to connect to rheological materials and this coincides with the later stages in the design process (Figure 1).

To allow for comparison of different material classes, early-stage rheological design targets would be ideally represented in terms of material properties (material functions). In the most general case, a specific constitutive model must be chosen to predict a nonlinear rheological response to nonhomogeneous deformation fields with complex time history (e.g., turbulent pipe flow). When and if a specific constitutive model must be chosen, then design freedom is fundamentally limited, since any particular constitutive equation does not apply across all material classes (polymers, colloids, composites, etc.)

To make such modeling efforts possible with material functions, the viscoelastic deformation in the system must either (i) match the deformation/loading protocol of a material function, or (ii) be linear viscoelastic. The first case requires that the deformation can be suitably approximated as either purely simple-shear or shear-free (extensional) flow, in which the time-dependent history matches that used for defining rheological material functions [11, 18]. These time-histories include step-rate startup flows, step-strain deformation, step-stress loading, oscillatory (vibratory) deformation, and steady-state flow.

The second case (our focus here) applies for any linear viscoelastic deformation, with any complex time-dependent history. Linear viscoelastic responses are described by experimentally measurable material functions that depend only on a timescale, e.g., the shear relaxation modulus $G(t)$. In this special regime, this material function is equivalent to a constitutive model parameter, and therefore applicable to any three-dimensional deformation history. For example, the Boltzmann superposition integral uses the same function $G(t)$, in tensorial form:

$$\underline{\underline{\sigma}}(t) = \int_{-\infty}^{t} G(t-t')\underline{\underline{\dot{\gamma}}}(t')dt', \tag{1}$$

where $\underline{\underline{\sigma}}(t)$ is the stress tensor, and the strain-rate tensor is

$$\underline{\underline{\dot{\gamma}}} = \underline{\nabla}\,\underline{v} + (\underline{\nabla}\,\underline{v})^{\mathrm{T}}, \tag{2}$$

where $\underline{v}$ is the velocity field. Equation (1) is limited to small deformation in the linear viscoelastic regime for incompressible materials, but applies for any linear viscoelastic material (polymer, colloid, gel, composite, etc.). The convolution integral of Eqn. (1) presents a challenge to optimizing the functional form of $G(t)$. In particular, governing equations such as conservation of momentum cannot be written as instantaneous functions of state variables, and this cannot be written in linear algebra matrix form. Instead, an integral over all past time is required.

The kernel function $G(t)$ is the most general design variable for linear viscoelastic materials (or alternatively creep compliance $J(t)$). A time-dependent Poisson ratio may also be considered, but we do not consider this additional degree of freedom here. In this work we consider incompressible materials, which are typically good approximations of soft or solvent-based viscoelastic materials such as elastomers, polymer melts, polymer solutions, and colloidal solutions, although hard materials and some foams are compressible, even with negative Poisson ratio [19].

In this work we will also consider 1-dimensional deformation, where Eqn. (1) reduces to a single scalar equation, rather than a tensor equation. We also make an analogy from intensive material properties (stress, strain-rate, modulus), to extensive properties (force, velocity, and stiffness) for application to viscoelastic structures. By analogy to Eqn. (1), the 1-D extensive expression for the force from a generalized viscoelastic structural element is

$$F_{VE}(t) = \int_{-\infty}^{t} G(t-t')\dot{x}(t')dt'., \tag{3}$$

where $\dot{x}$ is the velocity experienced by the element (dimensions $\dot{x}\doteq[\mathrm{LT}^{-1}]$) and $G(t-t')\doteq[\mathrm{FL}^{-1}]$). With a change of variable $s = t-t'$ this becomes

$$F_{VE}(t) = \int_{0}^{\infty} G(s)\dot{x}(t-s)ds. \tag{4}$$

3.1 Linear viscoelastic design can involve only one function

The relaxation modulus $G(t)$ in Eqn. (1) is an independent design parameter (a single-valued function). An alternative design parameter for linear viscoelasticity is the creep compliance $J(t)$, and an equation analogous to Eqn. (1) could be written in terms of the stress history $\underline{\underline{\sigma}}(t')$. The functions $G(t)$ and $J(t)$ are interrelated, and therefore not independent design functions. All of the linear viscoelastic material functions are interrelated [20], and therefore only one single-valued function can be specified in the design.

Importantly, some common linear viscoelastic material functions cannot be treated as independent design variables for modeling. In particular, this includes the dynamic oscillatory material functions. For example, the viscoelastic moduli $G'(\omega)$ and $G''(\omega)$ conceptually represent the elastic and viscous stress response, respectively, to imposed oscillatory deformation. For a viscoelastic fluid (with stress relaxing to zero at infinite time) these functions are directly related to $G(t)$ as

$$G'(\omega) = \omega\int_{0}^{\infty} G(s)\sin(\omega s)ds \tag{5}$$

$$G''(\omega) = \omega\int_{0}^{\infty} G(s)\cos(\omega s)ds. \tag{6}$$

Since each function is related to $G(t)$, the two functions cannot

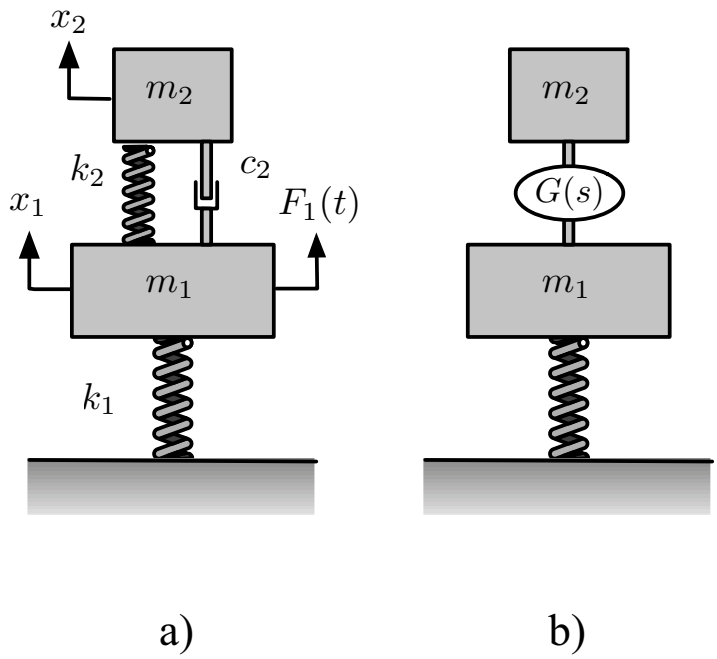

Figure 2: Design of optimal viscoelastic damping with either (a) the typical approach of a specific topological arrangement of springs and dashpots, or (b) a generalized linear viscoelastic element with relaxation modulus $G(s)$. The second approach increases design freedom and identifies more optimal design targets.

be independent. The interrelations are given by the Kramers-Kronig relations, shown most easily in terms of dynamic viscosities η' and η'' [18]

$$\eta''(\omega) = \frac{2\omega}{\pi}\int_0^\infty \frac{\eta'(x)}{\omega^2 - x^2}dx \tag{7}$$

$$\eta'(\omega) - \eta'(\infty) = \frac{2}{\pi}\int_0^\infty \frac{x\eta''(x)}{x^2 - \omega^2}dx \tag{8}$$

where

$$\eta''(\omega) = G'(\omega)/\omega \tag{9}$$

$$\eta'(\omega) = G''(\omega)/\omega. \tag{10}$$

Since dynamic moduli must satisfy the Kramers-Kronig relation, they are not independent design variables. This is true for any in-phase and out-of-phase dynamic material functions, including moduli G' and G'', viscosities η' and η'', compliances J' and J'', and fluidities ϕ' and ϕ''. The interdependence also limits the separate specification of frequency-dependent magnitude and phase angle.

3.2 Numerical optimization of $G(t)$

Any topological arrangement of springs and dashpots can be represented by a relaxation modulus such as $G(t)$. We wish to consider arbitrary functional forms of $G(t)$, and to integrate this into governing equations for dynamical systems involving designer viscoelastic materials or structures. Two features of $G(t)$ present numerical challenges that can be solved be restructuring this kernel function. The first challenge is the possibility of a superposed delta function (representing a dashpot in parallel), and the second is the possibility of a superposed constant (representing a spring in parallel). These are challenges to numerical optimization routines that must take numerical integrals of an arbitrary function $G(t)$, Eqn. (1).

These numerical issues are resolved by representing the general viscoelastic kernel function as

$$G(s) = G_\infty + \eta_0\delta(s) + G_{VEF}(s) \tag{11}$$

where G_∞ is the parallel spring constant, η_0 is the parallel dashpot coefficient, and $G_{VEF}(t)$ is for a general ViscoElastic Fluid (VEF), that excludes an instantaneous viscous response (delta function), and decays to zero at long times,

$$\lim_{s\to 0} G_{VEF}(s) = 0. \tag{12}$$

The numerical optimization parameters are then G_∞, η_0, and the function $G_{VEF}(s)$.

4 Example Problem: Dynamic Vibration Absorber

In many applications engineers seek to reduce mechanical vibration arising from rotating equipment, vortex shedding, or other sources of cyclic force input. Increasing mechanical rigidity is one approach for reducing vibration amplitude, but often is an unnecessarily expensive option. Passive vibration absorbers are a simple and inexpensive alternative solution for many applications.

Consider the model of a mechanical system in Fig. 2a. The primary system is represented by a mass (m_1) supported by a stiff spring (k_1). A cyclic force $F_1(t)$ applied to m_1 induces vibration in the system.

Vibrations can be damped by connecting a secondary mass m_2. The standard design problem might assume a simple combination of spring and dashpot in parallel (a Kelvin-Voigt viscoelastic model), as in Fig. 2a. With this specific topology of spring and dashpot, the two viscoelastic design variables are k_2 and c_2.

The viscoelastic connection can be generalized as (i) an arbitrary force trajectory for the connection, (ii) frequency-dependent spring and dashpot in parallel, or (iii) a generalized time (frequency) dependent linear viscoelastic element as in Fig. 2b, with the material function $G(s)$. We consider all three cases.

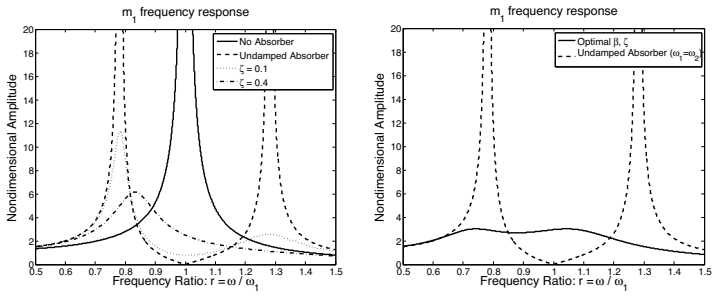

Figure 3: Response of system in Fig. 2a with $\mu = 0$ (no absorber), or $\mu = 0.25$ with $\beta = 1$.

4.1 Preliminaries

Fig. 3a illustrates the primary system vibration response over a range of frequencies. Here the abscissa is the ratio of the forcing frequency ω (assuming $F(t) = F_0 \sin(\omega t)$) to the natural frequency of the primary system $\omega_1 = \sqrt{k_1/m_1}$. The solid line shows how the non-dimensional amplitude of the primary system (i.e., $\hat{x}_1 = \frac{x_1 k_1}{F_0}$) with no absorber varies with forcing frequency. As we approach resonance ($\omega/\omega_1 = 1$), $\hat{x}_1$ approaches infinity. Increasing k_1 reduces the amplitude of x_1, but this requires more costly construction and does not eliminate resonant behavior. Alternatively, adding a vibration absorber to the primary system can reduce vibration amplitude significantly at low cost. One simple option for an absorber is to add a secondary sprung mass to the primary system, as shown in Fig. 2a. If m_2 is connected to m_1 via a parallel spring (k_2) and damper (c_2), as in Fig. 2a. A linear model for the complete system is:

$$\mathbf{M}\ddot{\mathbf{x}} + \mathbf{C}\dot{\mathbf{x}} + \mathbf{K}\mathbf{x} = \mathbf{F}, \tag{13}$$

where $\mathbf{M} = \begin{bmatrix} m_1 & 0 \\ 0 & m_2 \end{bmatrix}$ is the mass matrix, $\mathbf{C} = \begin{bmatrix} c_2 & -c_2 \\ -c_2 & c_2 \end{bmatrix}$ is the damping matrix, $\mathbf{K} = \begin{bmatrix} k_1 + k_2 & -k_2 \\ -k_2 & k_2 \end{bmatrix}$ is the stiffness matrix, $\mathbf{F} = [F_0 \sin \omega t, 0]^{\mathrm{T}}$ is the force vector, and $\mathbf{x} = [x_1, x_2]^{\mathrm{T}}$ are the position trajectories of m_1 and m_2. The analytical solution for the dimensionless amplitude of x_1 is:

$$\hat{x}_1 = \sqrt{\frac{(2\zeta r)^2 + (r^2 - \beta^2)^2}{(2\zeta r)^2 (r^2 - 1 + \mu r^2)^2 + (\mu r^2 \beta^2 - (r^2 - 1)(r^2 - \beta^2))^2}} \tag{14}$$

where $\mu = \frac{m_2}{m_1}$ is the mass ratio, $\beta = \frac{\omega_2}{\omega_1} = \sqrt{\frac{k_2 m_1}{k_1 m_2}}$ is the natural frequency ratio, $\zeta = \frac{c_2}{2 m_2 \omega_1}$ is the damping ratio, and $r = \frac{\omega}{\omega_1}$ is the frequency ratio [21].

We can tune an undamped ($c_2 = \zeta = 0$) vibration absorber such that it eliminates vibration at $r = 1$ (i.e., resonance of the primary system). From Eqn. (14) we can see that $\hat{x}_1 = 0$ at $r = 1$ if $\zeta = 0$ and $r = \beta$, or equivalently $\omega_1 = \omega_2$. This behavior is shown in Fig. 3a (dashed line), but amplitude increases significantly when r deviates from 1. This simple undamped absorber is only effective over a narrow frequency band. In many realistic conditions the actual vibration frequency varies over a wide range, motivating a different design that is more robust to frequency variations. Adding damping reduces amplitude at off-design frequencies, but increases the amplitude near $r = 1$, illustrated by the $\cdots$ and $- \cdot -$ curves in Fig. 3a. Thus, there is an inherent tradeoff in absorber design between amplitude minimization and robustness.

Stiffness and damping can be optimized together to minimize vibration amplitude over a range of frequencies. The solid line in Fig. 3b illustrates the frequency response that results when we minimize the maximum value of $\hat{x}_1$ over the range $0.5 \leq r \leq 1.5$ with respect to β and ζ (μ held fixed at 0.25). Robustness is improved over the damped absorber responses in Fig. 3a, but the maximum amplitude is still significant. Near $r = 1$ the tuned undamped absorber (dashed line in Figs. 3a and d) has much better response.

4.2 Arbitrary force-trajectory connection

Suppose for a moment that we could design an absorber where we make no assumptions regarding the nature of the connection between m_1 and m_2, i.e., our idealized vibration absorber is capable of supplying an arbitrary force $F_2(t)$ between m_1 and m_2. If the objective is to minimize $\hat{x}_1$ across a frequency range, choosing $F_2(t) = -F_1(t)$ for any given frequency will result in $\hat{x}_1 = 0$. This analytical result was used for numerical validation by minimizing $\hat{x}_1$ with respect to an arbitrary trajectory $F_2(t)$ using direct transcription (DT), an open-loop optimal control method based on nonlinear programming that is capable of solving for arbitrary force trajectories in more complicated systems without an analytical solution [16,22]. Implementing an absorber based on an optimal force trajectory might be possible using an active control system and a suitable actuator (e.g., [23, 24]), but this is a complicated and energy-intensive solution. Might it be possible to achieve the same result with a passive system? We posit that studying optimal arbitrary force trajectories can provide a basis for creative exploration of physically realizable design solutions.

Let us take one step closer to reality by exploring absorbers with a parallel spring-damper topology (Fig. 2a). From Eqn. (14), we can see that if $\zeta = 0$ and $r = \beta$, the response amplitude will be zero. We already observed from the tuned undamped absorber that if $\omega_1 = \omega_2$, the response will be zero at $r = 1$, but is non-zero if $r \neq 1$. If $r = 1$, then $\omega_1 = \omega_2$ implies that $r = \beta$ for an undamped system. But what about other frequencies? What kind of system would produce a zero response at any frequency? The optimal force trajectory $F_2(t) = -F_1(t)$ implies that the absorber needs to oscillate at the same frequency as the input force. This can be realized if the natural frequency of the absorber ω_2 can

be adjusted to match the input ω, which agrees with the above requirement that $\zeta = 0$ and $r = \beta$.

An optimal passive absorber needs a natural frequency that can vary with the forcing frequency, and has zero damping. Varying m_2 in real time is impractical, so that leaves us with developing an absorber system with variable stiffness.

4.3 Frequency-dependent spring and dashpot in parallel

Fortunately, materials do exist with stiffness that varies with frequency. We take one more step toward reality by considering an absorber with parallel spring/damper topology where stiffness and damping can vary arbitrarily with frequency. If we seek to minimize $\hat{x}_1$ across some range of forcing frequencies with respect to arbitrary (non-dimensional) stiffness and damping functions ($\beta(r)$ and $\zeta(r)$, respectively), as expected we discover that $\beta(r) = r$, $\zeta(r)$ is driven to zero, and $\hat{x}_1 = 0$ for any value of r.

If we look at this relationship using dimensional terms, $\beta = r$ is equivalent to $k_2 = m_2\omega^2$. We need an absorber material whose stiffness increases quadratically with frequency. Some viscoelastic materials do follow a power law relationship with frequency, inspiring another step toward a realistic physical model that still results in minimal primary system vibration.

$$\beta(r) = \beta_0 r^n \tag{15}$$

$$\zeta(r) = \zeta_0 r^n \tag{16}$$

Both functions are now parameterized by three constants: the coefficients β_0 and ζ_0, and the exponent n. $\beta(r)$ and $\zeta(r)$ are no longer arbitrary; they are coupled through n and can take on only limited shapes, but a significant amount of design freedom is still provided. The optimal response using this first power law model is shown in Fig. 4a (dashed line). The amplitude is zero for every frequency in the range displayed, the best possible result. The dashed line in Fig. 4b shows that the requirement $\beta(r) = r$ is satisfied, i.e., $n = 1$. Setting $n = 1$ enables ideal stiffness properties, but constrains the slope of $\zeta(r)$, shown by the dashed line in Fig. 4c. Damping is very small, but not quite zero due to numerical limitations, so $\hat{x}_1$ is only approximately zero.

This exercise helped us discover what properties an ideal viscoelastic structure (or material) must have to provide optimal absorber performance. It considered only the specific topological arrangement of a spring and dashpot in parallel (i.e. a Kelvin-Voigt topology), but allowed for frequency-dependence unconstrained by the Kramers-Kronig relation [Eqn. (7)–(8)]. We can represent viscoelastic structures and materials more realistically, yet generally, by using a relaxation modulus kernel function, $G(s)$, which we consider in the next section.

4.4 Generalized viscoelastic connection $G(s)$

The Boltzmann constitutive equation can represent any arbitrary topological arrangement of springs and dashpots. We will consider the 1-D mechanical force version of this expression, Eqn. (4). In this case the design variable is a single-valued function $G(s)$.

Given an initial condition $F_{ve}(t = 0) = 0$, Eqn. (4) has limits of integration from 0 to t. In general, the expression requires convolution of the kernel function $G(s)$ with the entire time-history of the velocity experienced by the element, $\dot{x}(t)$.

For the particular system in Fig. 2b, with generalized viscoelastic damping and the initial condition $F_{ve}(t = 0) = 0$, the governing equations for conservation of linear momentum are most generally written as

$$-\int_0^t G(s)\left[\dot{x}_1(t-s) - \dot{x}_2(t-s)\right] ds + m_2\ddot{x}_2(t) = 0 \tag{17}$$

for m_1, and for m_2

$$\int_0^t G(s)\left[\dot{x}_1(t-s) - \dot{x}_2(t-s)\right] ds + k_1 x_1(t) + m_1\ddot{x}_1(t) = F_0 \sin\omega t. \tag{18}$$

The convolution integral structure has two important consequences. First, the equations cannot be written in matrix form. Second, the numerical simulation of this model requires increased computation at each time step, since each step requires an integration of the entire prior time-history of velocities.

The particular situation here can be simplified by considering time-periodic limit cycle behavior, when the system has reached an alternance state. For this linear system with sinusoidal forcing $F_1(t) = F_0 sin\omega t$, the steady-state displacement response of $x_1(t)$ and $x_2(t)$ will be time-periodic at the forcing frequency [21]. The known structure of this harmonic solution will simplify the convolution integral terms, to an extent that we *can* write the governing equations as a function of instantaneous state variables. We will see that integral calculations of $G(s)$ terms are not required at each time step.

Using complex notation, the displacements of the masses have the form

$$x_1(t) = \mathrm{Im}\left\{x_1^* e^{i\omega t}\right\} \tag{19}$$

$$x_2(t) = \mathrm{Im}\left\{x_2^* e^{i\omega t}\right\} \tag{20}$$

where Im$\{\}$ takes the imaginary portion of the complex quantity. The coefficients are

$$x_1^* = x_{1R} + ix_{1i} \tag{21}$$

$$x_2^* = x_{2R} + ix_{2i} \tag{22}$$

This assumed structural form will remove the convolution integral.

By substituting Eqns. (19)–(22) into Eqns. (17)–(18), a linear system of four equations and four unknowns will result. The system of equations takes the form

$$\mathbf{Ax} = \mathbf{B}. \tag{23}$$

The unknowns are

$$\mathbf{x} = [x_{1R}, x_{1i}, x_{2R}, x_{2i}]^{\mathrm{T}}. \tag{24}$$

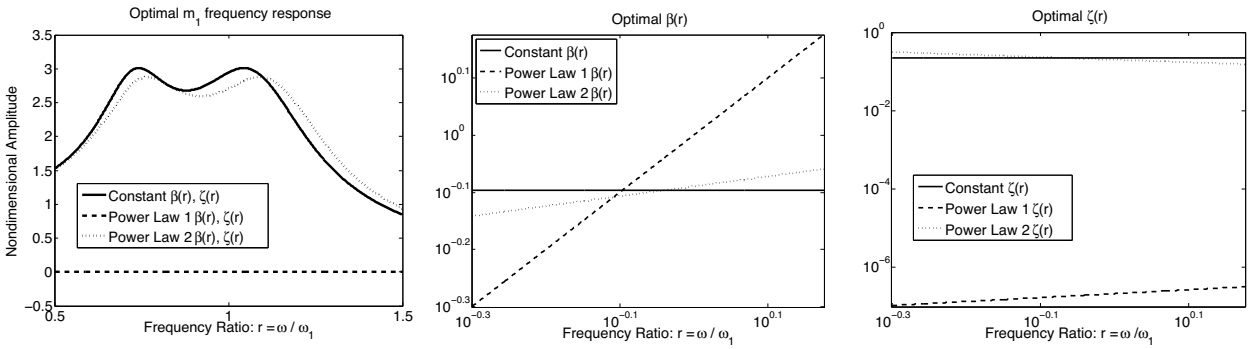

Figure 4: Optimal responses from power-law spring and dashpot arranged in parallel (Kelvin-Voigt type model), with no restriction on the power law exponent.

The nonhomogeneous portion is

$$\mathbf{B} = [F_0, 0, 0, 0]^{\mathrm{T}} \tag{25}$$

and the 4 by 4 matrix is given by $\mathbf{A} =$

$$\begin{bmatrix} (\omega S + k_2 + k_1 - m_1\omega^2) & (-\omega C - \omega c_2) & (-\omega S - k_2) & (\omega C + \omega c_2) \\ (-\omega C - \omega c_2) & (-\omega S - k_2 - k_1 + m_1\omega^2) & (\omega C + \omega c_2) & (\omega S + k_2) \\ (-\omega S - k_2) & (\omega C + \omega c_2) & (\omega S + k_2 - m_2\omega^2) & (-\omega C - \omega c_2) \\ (-\omega C - \omega c_2) & (-\omega S - k_2) & (\omega C + \omega c_2) & (\omega S + k_2 - m_2\omega^2) \end{bmatrix} \tag{26}$$

The scalar coefficients C and S require integral calculations that depend on the kernel function $G(s)$,

$$C(\omega) = \int_0^\infty G(s)\cos(\omega s)ds \tag{27}$$

$$S(\omega) = \int_0^\infty G(s)\sin(\omega s)ds. \tag{28}$$

Comparing this result to Eqn. (5) and Eqn. (6) shows that these integrals are related to the dynamic material function as

$$C = G''(\omega)/\omega = \eta'(\omega) \tag{29}$$

$$S = G'(\omega)/\omega = \eta''(\omega). \tag{30}$$

The primary design variable is still $G(s)$, since it gives the rheological signature of both dynamic moduli, and the dynamic moduli are not independent parameters due to the Kramers-Kronig relations in Eqs. (7)–(8).

Eqns. (23)–(28) are used to model the system of Fig. 2b, and to optimize the response of x_1^* in terms of the kernel function $G(s)$. The function $G(s)$ could be treated as a function of unknown structure, or a vector with specified point density where each value is independent of the others. Passive materials and systems would require a monotonically decreasing $G(s)$, but active systems (such as actuators or active biological materials) could be more complex. An arbitrary structure would also require numerical integration of Eqns. (27)–(28).

Here we parameterize the $G(s)$ curve with a finite number of parameters, and consider specific models for $G(s)$. From Eqn. (12), we will always include the scalar design parameters G_∞ and η_0; we then only need to consider the structural form of $G_{VEF}(s)$. We first consider the Kelvin-Voigt parameters only, equivalent to the standard problem as shown in Fig. 2a. This is defined by

$$G_{VEF}(s) = 0. \tag{31}$$

For this model, the dynamic moduli are simply given by

$$G'(\omega) = G_\infty \tag{32}$$

$$G''(\omega) = \eta_0\omega. \tag{33}$$

We also consider a generalized (multi-mode) Maxwell model, also known as a Prony series. This is defined by

$$G_{VEF}(s) = \sum_{k=1}^{N} G_k e^{-t/\lambda_k}. \tag{34}$$

Here will consider the cases of $(N = 1, 3, 5)$ in order to limit the optimization routine to a finite number of parameters (10 total parameters with $N = 5$). For this form, the total dynamic moduli are

$$G'(\omega) = G_\infty + \sum_{k=1}^{N} G_k \frac{(\lambda_k\omega)^2}{1 + (\lambda_k\omega)^2} \tag{35}$$

$$G''(\omega) = \eta_0\omega + \sum_{k=1}^{N} G_k \frac{\lambda_k\omega}{1 + (\lambda_k\omega)^2}. \tag{36}$$

Using a generalized Maxwell model, a very large number of parameters may be required to describe some functional forms of $G_{VEF}(s)$, such as power laws. Yet, power-law rheology is an important signature, seen in materials near a gel point [25, 26], and active biological materials such as cells [27]. In order to consider this broader design space, but with a small number of parameters, we will consider the critical gel model described by

$$G_{VEF}(s) = St^{-n} \tag{37}$$

where S is the gel strength parameter and n is the power-law coefficient. The exponent is typically $n \approx 1/2$, but more generally

is restricted to the range $0 < n < 1$. This bound on n prevents us from achieving the ideal stiffness relationship of $k_2 = m_2\omega^2$. The total dynamic moduli for the critical gel structural form are given by

$$G'(\omega) = G_\infty + G'_{CG}(\omega) \tag{38}$$

$$G''(\omega) = \eta_0\omega + G''_{CG}(\omega) \tag{39}$$

The critical gel dynamic moduli are given by [25, 26, 28]:

$$G'_{CG}(\omega) = \frac{G''_{CG}(\omega)}{\tan\left(n\frac{\pi}{2}\right)} = \Gamma(1-n)\cos\left(\frac{n\pi}{2}\right) S\omega^n \tag{40}$$

where $\Gamma(\cdot)$ is the Gamma function. The first equality of Eqn. (40) links stiffness and damping, further constraining viscoelastic properties differently than assumed in the previous section. Note that $G''(\omega)$ and $G'(\omega)$ have equal slope for a given n (i.e., the modulus lines are parallel).

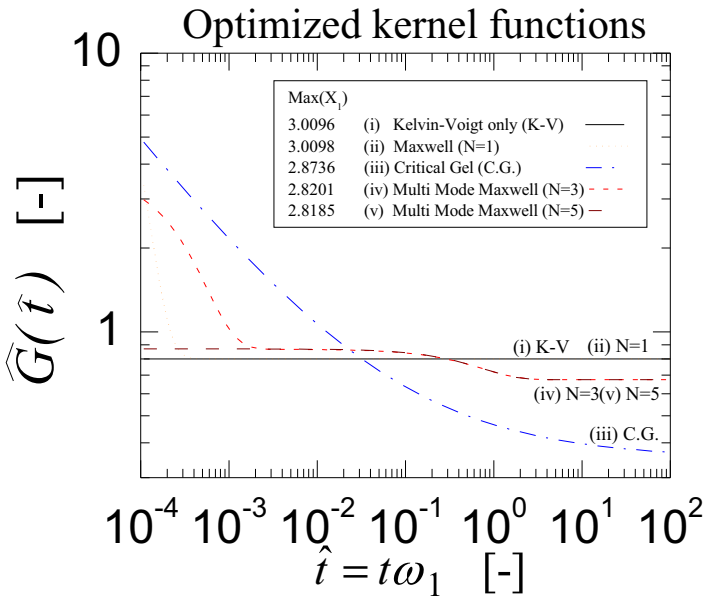

Figure 5: Optimized dimensionless kernel functions $\hat{G}(s) \equiv G(s)/k_1$ for a structural viscoelastic connection with different functional forms of $G_{VEF}(s)$ (Figure 2b with $\mu = 0.25$). Except for (iii) Critical Gel, all models contain a delta function at $s = 0$ corresponding to a dashpot in parallel.

We optimized the different forms of the kernel function in order to minimize the peak amplitude of $x_1(\omega)$ across the range of frequency ω. Optimization is performed using the MATLAB™ optimization toolbox with the function 'fmincon'. The results for the optimal viscoelastic kernel functions are presented in dimensionless form and are shown in Table 1. Using the primary

Model	Max($\hat{x}_1$)[-]	$\hat{G}_\infty$ [-]	$\hat{\eta}_0$ [-]	VEF parameters [-]	
Kelvin-Voigt	3.0096	0.16	0.1102	-	-
Maxwell (N=1)	3.0098	0.1599	0.1099	$\hat{\eta}_1 = 0.0013$	$\hat{\lambda}_1 = 0.00004$
Multimode Maxwell (N=3)	2.8201	0.1136	0.0005	$\hat{\eta}_1 = 0.001$ $\hat{\eta}_2 = 0.1305$ $\hat{\eta}_3 = 0.1405$	$\hat{\lambda}_1 = 0.00035$ $\hat{\lambda}_2 = 0.6769$ $\hat{\lambda}_3 = 767.0082$
Multimode Maxwell (N=5)	2.8185	0.1134	0.0005	$\hat{\eta}_1 = 0.00001$ $\hat{\eta}_2 = 0.0025$ $\hat{\eta}_3 = 0.0847$ $\hat{\eta}_4 = 0.1290$ $\hat{\eta}_5 = 0.4784$	$\hat{\lambda}_1 = 0.0156$ $\hat{\lambda}_2 = 0.6716$ $\hat{\lambda}_3 = 850.9421$ $\hat{\lambda}_4 = 0.6747$ $\hat{\lambda}_5 = 20216.22$
Critical Gel	2.8736	0.0312	0	S=0.1119	n=0.4030

Table 1: Optimized parameters for kernel functions $G(s)$ for different functional forms of $G_{VEF}(s)$.

spring stifffness k_1 and natural frequency of the primary system $\omega_1 = \sqrt{\frac{k_1}{\omega_1}}$, we define a dimensionless moduli $\hat{G}(s) \equiv G(s)/k_1$ and dimensionless timescales $\hat{t} \equiv t\omega_1$ and $\hat{\lambda} \equiv \lambda\omega_1$. The nondimensional amplitude of the primary system remains $\hat{x}_1 \equiv \frac{x_1 k_1}{F_0}$ and a nondimensional damper viscosity can be defined as $\hat{\eta}_0 \equiv \frac{\eta_0\omega_1}{k_1}$. Fig. 5 shows the full form $\hat{G}(s)$ from Eqn. (12), which includes the parameters $\hat{G}_\infty$ and $\hat{\eta}_0$. The parameter $\hat{\eta}_0$ would appear as a delta function in $\hat{G}(s)$ at $s = 0$, which cannot be shown in Fig. 5. The effect of η_0 can be easily shown with a plot of dynamic moduli, with the signature $G''(\omega) \sim \eta_0\omega$. The dimensionless dynamic structural moduli corresponding to the optimial $\hat{G}(s)$ kernel functions are given in Fig. 6.

The maximum amplitudes are shown in Table 1. The peak amplitude decreases by considering more general viscoelastic structures compared to the Kelvin-Voigt structure. Surprisingly, adding a single-mode Maxwell model, with two extra design parameters, offers no improvement. This similarity is evident in the overlapping forms of the optimum kernel functions for these two models. The additional Maxwell element, at optimal conditions, is simply an additional dashpot (or an additional spring as we observed in some optimization runs), but the total structure is effectively the same as the optimal Kelvin-Voigt parameters.

The critical gel model improves the performance, with power-law coefficient $n = 0.4030$. For the critical gel model we find $\eta_0 = 0$ an optimal value, and a finite but comparatively smaller value for G_∞.

We find additional performance enhancement with more degrees of freedom for shaping the stress relaxation function $G(s)$, by using a multi-mode Maxwell model. The optimial peak amplitude of $\hat{x}_1$ is the same for $N = 3$ and $N = 5$. With an increasing

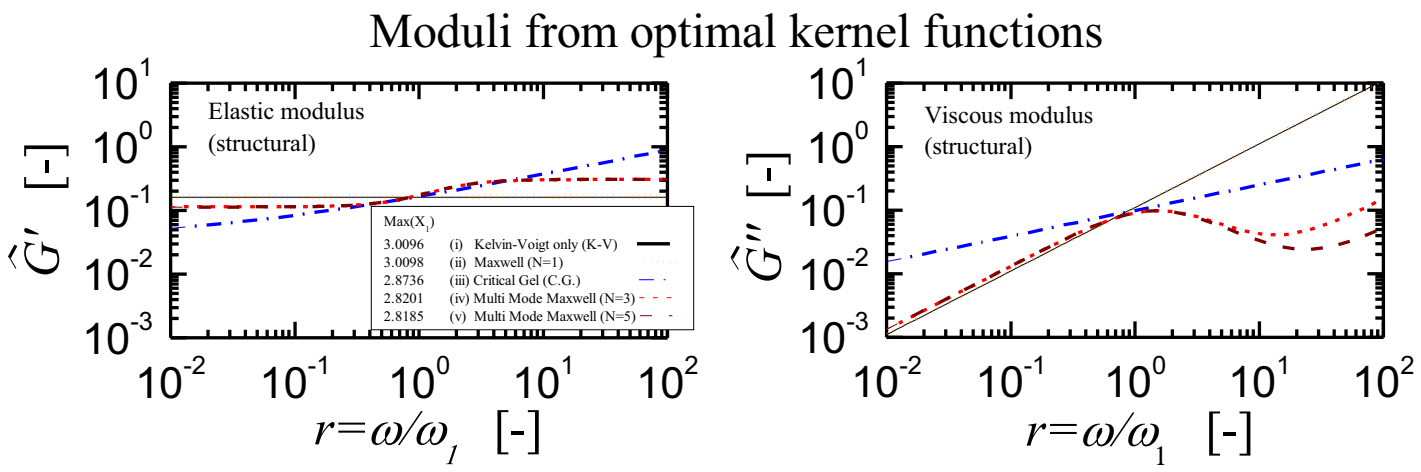

Figure 6: Structural dynamic moduli from the optimized kernel functions of Fig. 5.

number of parameters the optimization tasks become increasingly complex, and more robust optimization routines will be needed.

In this example we find that the most ideal rheological design target involves time-dependent viscoelastic behavior, specifically for a multi-mode Maxwell element ($N = 3$ or $N = 5$) in parallel with a Kelvin-Voigt element (spring and dashpot in parallel). The response is also improved with a critical gel model, suggesting that critical gel materials could be very useful in vibrational damping, and perhaps of increasing benefit in more complex systems with force inputs at multiple frequencies.

These results could not be identified by simply representing viscoelastic damping as a fixed amplitude and phase across the range of frequency. In fact, such a statement could potentially violate the Kramers-Kronig relations of Eqns. (7)–(8). For the simple geometry and forcing input of Fig. 2, the generalized viscoelastic conditions are modest improvements to the optimized Kelvin-Voigt model. For more complex arrangements, unsteady oscillations, and force inputs that superpose different frequencies, viscoelastic elements can still be modeled with our methodology described here. In cases both simple and complex, the early-stage target setting will provide valuable insights. Ideal design targets can be set, and when compared to currently available materials, the targets will guide the direction of novel material design.

5 Conclusions

In this work we have described a methodology for the early-stage design of rheologically-complex materials. We outline criteria for using rheological material functions directly in mathematical models. Here we have focused on the case of linear viscoelastic deformations, for which a single function $G(s)$ (or its corallary function $J(s)$) is the design variable.

An example problem was considered with steady-state harmonic vibration. The convolution integrals were then simplified so that an instantaneous state-space representation could be used for the governing equations. In general this may not be the case, and the full convolution integrals may be needed in the simulation of a linear viscoelastic system with complex deformation history or nonhomogeneous deformation.

If deformations are too complex to use material functions, then the only option is to directly specify a constitutive model. One may be able to optimize the constants of a constitutive model, but this sacrifices design freedom, since not all materials will obey a given constitutive model, even though the material may provide a useful rheological response.

Designers will not necessarily progress from high to low design freedom studies in a linear fashion. After exploring in detail one material type, designers may gain some insights that motivate additional studies at a higher design freedom level. We expect the process to be iterative and nonlinear, but guided by the general modeling rules and methodology that we have initiated here.

The methodology outlined here will help identify early-stage design targets that are independent of material class, such as $G(s)$. By choosing a material function as a design target, the rheological material designer can choose from the entire toolbox of complex materials, including polymers, colloids, gels, composites, etc. It may sometimes occur that available materials do not achieve optimal target properties but materials with the most promising properties can be modeled in terms of their measured rheological material functions. Functionality driven multi-level modeling methods such as inductive design exploration [10] will

be useful in such cases, but the challenge will be to manage function-valued properties e.g. $G(t)$ rather than scalar single valued properties. Still, if the optimal target cannot be achieved with available materials, the optimal target will remain a guide for any future materials development.

We expect that linear viscoelastic design will be applicable to any system in which any topological arrangement of linear springs and dashpots can be assumed, or materials are used within the linear viscoelastic limit of deformation. Cyclic loading situations are particularly amenable to these techniques, including locomotion dynamics of robotics and prosthetics, energy harvesting, and energy conversion, and we expect a wide range of soft material design opportunities that will benefit from early-stage rheological design targets.

REFERENCES

[1] Shadwick, R. E., 1999. "Mechanical design in arteries". *Journal of Experimental Biology,* **202**(23), pp. 3305–3313.

[2] Denny, M. W., 1980. "The role of gastropod pedal mucus in locomotion". *Nature,* **285**(5761), pp. 160–161.

[3] Ewoldt, R. H., Clasen, C., Hosoi, A. E., and McKinley, G. H., 2007. "Rheological fingerprinting of gastropod pedal mucus and synthetic complex fluids for biomimicking adhesive locomotion". *Soft Matter,* **3**(5), pp. 634–643.

[4] Ewoldt, R. H., Hosoi, A. E., and McKinley, G. H., 2009. "Nonlinear viscoelastic biomaterials: meaningful characterization and engineering inspiration". *Integrative and Comparative Biology,* **49**(1), pp. 40–50.

[5] Cussler, E. L., and Moggridge, G. D., 2012. "A changing chemical industry". *Reviews in Chemical Engineering,* **28**(2-3), Jan., pp. 73–79.

[6] Linsey, J. S., Tseng, I., Fu, K., Cagan, J., Wood, K. L., and Schunn, C., 2010. "A Study of Design Fixation, Its Mitigation and Perception in Engineering Design Faculty". *Journal of Mechanical Design,* **132**(4), p. 041003.

[7] Ulrich, K., 2012. *Product design and development*, 5th ed. McGraw-Hill, New York.

[8] Kim, H. M., Michelena, N. F., Papalambros, P. Y., and Jiang, T., 2003. "Target cascading in optimal system design". *Journal of Mechanical Design,* **125**(3), p. 474. ID: 4657327639.

[9] Kim, H. M., Rideout, D. G., Papalambros, P. Y., and Stein, J. L., 2003. "Analytical target cascading in automotive vehicle design". *Journal of Mechanical Design,* **125**(3), p. 481. ID: 4657327657.

[10] Choi, H., McDowell, D. L., Allen, J. K., Rosen, D., and Mistree, F., 2008. "An inductive design exploration method for robust multiscale materials design". *Journal of Mechanical Design,* **130**(3), MAR 2008, p. 031402.

[11] Dealy, J. M., 1995. "Official nomenclature for material functions describing the response of a viscoelastic fluid to various shearing and extensional deformations". *Journal of Rheology,* **39**(1), pp. 253–265.

[12] Johnson, C. D., 1995. "Design of Passive Damping Systems". *Journal of Mechanical Design,* **117**(B), p. 171.

[13] Hilton, H. H., and Yi, S., 1992. "Analytical formulation of optimum material properties for viscoelastic damping". *Smart Materials and Structures,* **1**(2), p. 113.

[14] Hilton, H. H., 2005. "Optimum linear and nonlinear viscoelastic designer functionally graded materials - Characterizations and analysis". *Composites Part A: Applied Science and Manufacturing,* **36**(10), pp. 1329–1334.

[15] Hilton, H. H., Lee, D. H., and El Fouly, A. R. A., 2008. "Generalized viscoelastic designer functionally graded auxetic materials engineered/tailored for specific task performances". *Mechanics of Time-Dependent Materials,* **12**(2), pp. 151–178.

[16] Allison, J. T., Kaitharath, A., and Herber, D. R., 2012. "Wave Energy Extraction Maximization Using Direct Transcription". In The Proceedings of the ASME 2012 International Mechanical Engineering Congress & Exposition, ASME.

[17] Allison, J. T., and Han, Z., 2011. "Co-Design of an Active Suspension Using Simultaneous Dynamic Optimization". In The Proceedings of the ASME 2011 Design Engineering Technical Conferences & Computers and Information in Engineering Conference, no. DETC2011-48521, ASME.

[18] Bird, R. B., Armstrong, R. C., and Hassager, O., 1987. *Dynamics of Polymeric Liquids: Volume 1 Fluid Mechanics*, 2nd ed. John Wiley and Sons, Inc, New York.

[19] Lakes, R., 1987. "Foam Structures with a Negative Poisson's Ratio.". *Science,* **235**(4792), pp. 1038–40.

[20] Ferry, J. D., 1980. *Viscoelastic properties of polymers*, Vol. 3d. Wiley.

[21] Inman, D. J., 2001. *Engineering Vibration*, 2nd ed. Prentice-Hall, Inc.

[22] Biegler, L. T., 2010. *Nonlinear Programming: Concepts, Algorithms, and Applications to Chemical Processes*. SIAM.

[23] Jones, W. D., 2005. "Easy ride: Bose Corp. uses speaker technology to give cars adaptive suspension". *Spectrum, IEEE,* **42**(5), May, pp. 12–14.

[24] Gysen, B., and Paulides, J., 2010. "Active Electromagnetic Suspension System for Improved Vehicle Dynamics". *IEEE Transactions on Vehicular Technology,* **59**(3), pp. 1156–1163.

[25] Winter, H. H., and Chambon, F., 1986. "Analysis of linear viscoelasticity of a cross-linking polymer at the gel point". *Journal of Rheology,* **30**(2), Apr., pp. 367–382.

[26] Winter, H. H., and Mours, M., 1997. "Rheology of polymers near liquid-solid transitions". In *Neutron Spin Echo Spectroscopy, Viscoelasticity, Rheology (Advances in Polymer Science)*, Vol. 134. Springer Berlin, Heidelberg, pp. 165–234.

[27] Kollmannsberger, P., and Fabry, B., 2011. "Linear and Nonlinear Rheology of Living Cells". *Annual Review of Materials Research,* **41**(1), Aug., pp. 75–97.

[28] Chambon, F., and Winter, H. H., 1987. "Linear viscoelasticity at the gel point of a cross-linking PDMS with imbalanced stoichiometry". *Journal of Rheology,* **31**(8), Nov., pp. 683–697.